ELSEVIER

Journal of Organometallic Chemistry 558 (1998) 181–188

Journal of Organo metallic Chemistry

Synthesis and characterization of ethylene-bridged 1-*tert*-butyldimethylsiloxy-substituted bis(indenyl) and bis(tetrahydroindenyl)zirconium dichlorides

Reko Leino [a],*, Hendrik J.G. Luttikhedde [a], Ari Lehtonen [b], Peter Ekholm [a], Jan H. Näsman [a]

[a] *Department of Polymer Technology, Åbo Akademi University, FIN-20500, Åbo, Finland*
[b] *Department of Chemistry, University of Turku, FIN-20500, Turku, Finland*

Received 13 November 1997

Abstract

The synthesis and characterization of three siloxy-substituted zirconocene complexes *rac*- and *meso*-ethylenebis[1-(*tert*-butyldimethylsiloxy)indenyl]zirconium dichlorides (**3a**,**3b**) and *rac*-ethylenebis[1-(*tert*-butyldimethylsiloxy)-4,5,6,7-tetrahydroindenyl]zirconium dichloride (**4**) are reported. The molecular structures of **3b** and **4** have been determined and reveal that **3b** crystallizes in a chiral staggered *meso*-conformation, whereas **4** adopts the expected C_2 symmetric bent metallocene structure with indenyl-forward conformation of the ligand backbone. In both complexes **3b** and **4** the intramolecular oxygen-chlorine distances (3.15–3.30 Å) are close to the sum of their van der Waals radii (3.20 Å). © 1998 Elsevier Science S.A. All rights reserved.

Keywords: Indenyl; Zirconium; *ansa*-Metallocene; Siloxy

1. Introduction

Modification of chiral *ansa*-metallocene catalysts [1] with Lewis-basic functionalities is desirable in order to stabilize the cationic active sites essential for α-olefin coordination and chain propagation reaction. Until recently, direct hetero atom substitution of group IV metallocene complexes has, however, remained rare. The preparation of bis(dimethylaminocyclopentadienyl)titanocene was reported in 1984 [2]. Bis(2-aminoindenyl)zirconocene analogues have been prepared recently by several groups [3]. Disiloxane bridged bis(cyclopentadienyl) [4] and bis(indenyl) [5] zirconocenes, as well as pyridine bridged zirconocenes and hafnocenes [6] have been described. The presence of N–Zr interaction in the latter complexes has been reported to favor the formation of zirconocene cations [6].

In our earlier studies [7], we have shown that chiral 2-siloxy-substituted bis(indenyl) *ansa*-metallocenes form, in combination with MAO or other activators, highly active catalyst systems for homo- and copolymerization of α-olefins. A systematic variation of substitution patterns of these and other metallocenes is needed for delineation of spatial requirements and optimization of electronic properties for the catalytic applications. Therefore, we have also prepared some 1-siloxy-substituted analogues of the previously reported complexes, and describe here the synthesis and characterization of *rac*-(**3a**) and *meso*-(**3b**) [ethylenebis(1-(*tert*-butyldimethylsiloxy)-3-indenyl)]zirconium dichlorides, *rac*-[ethylenebis(1-(*tert*-butyldimethylsiloxy)-4,5,6,7-tetrahydro-3-indenyl)]zirconium dichloride (**4**), and the molecular structures of **3b** and **4**.

---

* Corresponding author. Fax: +358 2 2154866; e-mail: reko.leino@abo.fi

PII S0022-328X(98)00375-1

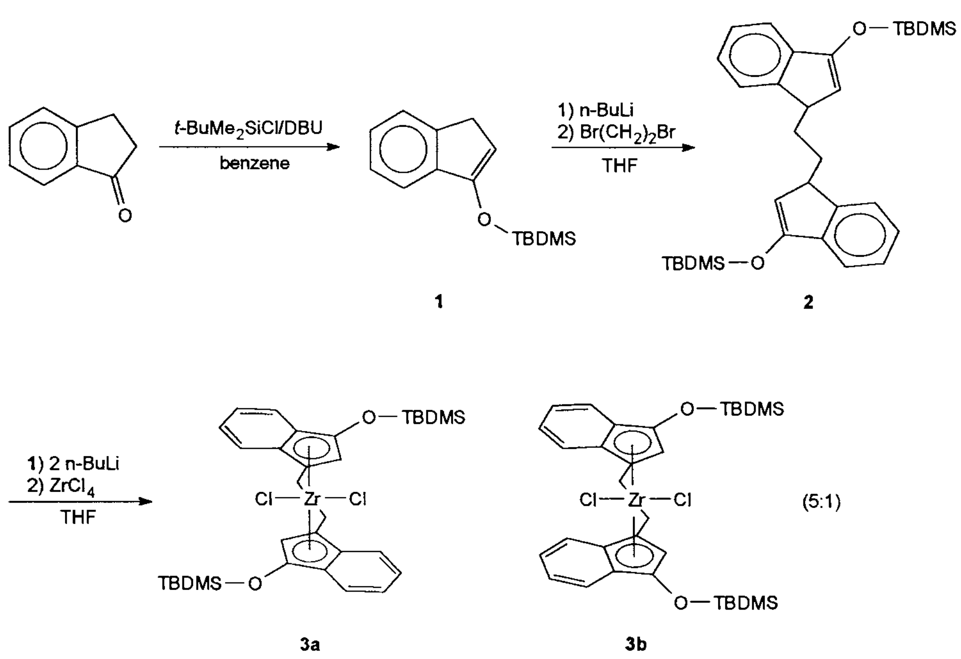

Scheme 1.

2. Results and discussion

As shown in Scheme 1, the reaction of 1-indanone with *tert*-butyldimethylchlorosilane and DBU in benzene gave 3-(*tert*-butyldimethylsiloxy)indene (**1**) in 92% yield. Deprotonation of **1** with *n*-BuLi and subsequent reaction of the lithium salt with dibromoethane in THF gave diastereomeric bis(3-(*tert*-butyldimethylsiloxy)indenyl)ethane (**2**) in 63% yield. Reaction of **2**-Li_2 with $ZrCl_4$ in THF gave, after Et_2O extraction and crystallization, **3** · 2THF in 22% yield. The product is formed in a *rac*:*meso* ratio of 5:1, as determined by ^1H NMR. Samples of the pure racemic diastereomer **3a** were obtained by careful recrystallization from toluene. Extraction of the evaporated mother liquor and Et_2O insolubles with CH_2Cl_2 gave, after concentration and crystallization, a small amount of the pure *meso* diastereomer **3b**, that was further purified by recrystallization from toluene. As shown in Scheme 2, catalytic hydrogenation of a 9:1 mixture of **3a** and **3b**, obtained by recrystallization of the original mixture, gave a similar ratio of the corresponding tetrahydroindenyl complexes in 84% yield. The pure racemic diastereomer **4** was obtained by careful recrystallization from hexane.

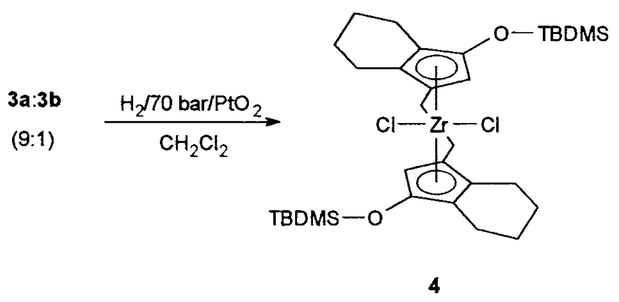

Scheme 2.

The ^1H and ^{13}C NMR spectra of **3a** and **4** are consistent with the expected C_2 symmetry. The H_α-protons of the five-membered rings show single resonances in ^1H NMR at 5.60 ppm (**3a**) and 4.96 ppm (**4**), respectively. The chemical shifts are shielded considerably compared to those of *rac*-Et(Ind)$_2$ZrCl$_2$ (6.20 ppm) [8] and *rac*-Et(IndH$_4$)$_2$ZrCl$_2$ (5.61 ppm) [9]. The *meso*-diastereomer **3b** gives a highly symmetric ^1H NMR spectrum indicating rapid conformational interconversion. Shielding of the H_α-resonance (5.72 ppm), compared to the corresponding value for *meso*-Et(Ind)$_2$ZrCl$_2$ (6.55 ppm) [8], indicates increased electron density in the five-membered ring.

The stereochemistries of **3b** and **4** were confirmed by X-ray structure determination. Despite several attempts, crystals suitable for X-ray analysis could not be obtained from **3a**. The molecular structures of **3b** and **4** are displayed in Figs. 1 and 2, respectively, with selected bond lengths and angles in Tables 1 and 2. A comparison of selected bonding parameters for seven different siloxy-substituted bis(indenyl) and bis(tetrahydroindenyl) *ansa*-zirconocenes is shown in Table 3.

3b crystallizes in a chiral staggered conformation as observed previously for other ethylene-bridged *meso*-bis(indenyl) and bis(tetrahydroindenyl) *ansa*-zirconocenes [3]d, [8,10,11]. The *R*,*S* stereoisomer, shown in Fig. 1, has a λ conformation of the Zr–C(1)–C(10)–C(11)–C(12) metallacycle. The two Zr–Cl bonds are not related by symmetry, and their local environments and hence the two coordination sites are dissimilar. The

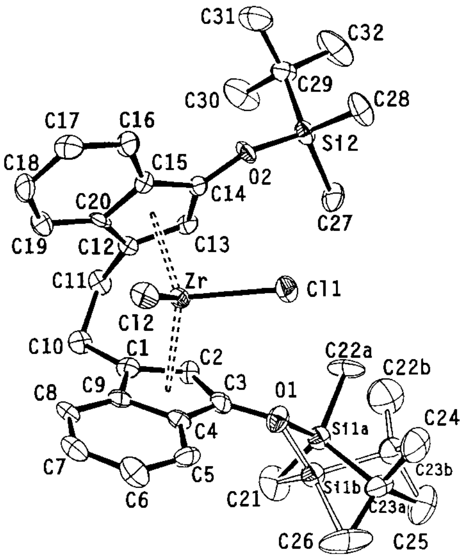

Fig. 1. Molecular structure of **3b**. Thermal ellipsoids are drawn at 20% probability level.

indenyl ligands take more space around the Zr atom than in racemic ethylenebis(indenyl) and ethylenebis(-tetrahydroindenyl) zirconium dichlorides [3]a, [7–9,11,12], as shown by the large angle between the Cp planes [64.6(4)°] and decreased Cl–Zr–Cl angle [96.19(11)°]. The ηC–O bond lengths of **3b** [1.341(12) Å] are slightly shorter than those of the racemic siloxy-substituted complexes [1.355(3)–1.376(4) Å].

Table 1
Selected bond distances (Å) and angles (°) for **3b**[a,b]

Intramolecular distances			
Zr–Cl(1)	2.426(3)	Zr–Cl(2)	2.435(3)
Zr–C(1)	2.444(10)	Zr–C(12)	2.465(9)
Zr–C(2)	2.499(9)	Zr–C(13)	2.530(10)
Zr–C(3)	2.622(11)	Zr–C(14)	2.627(10)
Zr–C(4)	2.661(11)	Zr–C(15)	2.632(11)
Zr–C(9)	2.583(10)	Zr–C(20)	2.525(11)
C(3)–O(1)	1.341(12)	C(14)–O(2)	1.341(12)
Zr–Cen(1)	2.255	Zr–Cen(2)	2.249
Intramolecular angles			
Cl(1)–Zr–Cl(2)	96.19(11)	Cen(1)–Zr–Cen(2)	126.4
Cp(1)–Cp(2)[b]	64.6(4)		

[a] Cen(1) and Cen(2) refer to the centroids of the C_5 rings with the lowest and highest crystallographic numbering, respectively.
[b] Angle between the cyclopentadienyl planes.

Complex **4** adopts the characteristic bent metallocene structure with crystallographically imposed C_2 symmetry. The stereoisomer shown in Fig. 2 has an *R*,*R* configuration of the bridgehead carbon atoms and a δ conformation of the Zr–C(1)–C(10)–C(10)*–C(1)* metallacycle. **4** crystallizes in the indenyl-forward conformation [8], as observed previously for several ethylene-bridged bis(indenyl) and bis(tetrahydroindenyl) group IV *ansa*-metallocene dichlorides [3]a, [7]d, [8,9,11,12]. The Zr–Centroid distance [2.2384(4) Å], Centroid–Zr–Centroid angle [126.43(2)°] and Cl–Zr–Cl angle [98.73(6)°] of **4** deviate slightly from those of the 2-substituted analogue, *rac*-Et[2-(*t*-BuMe$_2$SiO)IndH$_4$)]$_2$ZrCl$_2$, [Zr–Cen, 2.2307 Å; Cen–Zr–Cen, 125.24°; Cl–Zr–Cl, 98.16(6)°] [7]b. The trend in the Zr–C bond lengths of **4** [Zr–C(3), Zr–C(4) > Zr–C(9) > Zr–C(2), Zr–C(1); see Fig. 2 for numbering scheme] is similar to that observed by Ewen for *rac*-Et(3-MeInd)$_2$ZrCl$_2$ [12]. The corresponding bond lengths of *rac*-Et[2-(*t*-BuMe$_2$SiO)IndH$_4$)]$_2$ZrCl$_2$ [7]b show considerably less variation ranging from 2.502(4)–2.581(4) Å [for **4**: Zr–C = 2.465(3)–2.633(3) Å]. In **4**, the angle between the cyclopentadienyl planes (63.59°) is larger than those observed for the 2-siloxy-substituted complexes (57.7–61.0°) [7] and is, in fact, larger than the values

Table 2
Selected bond distances (Å) and angles (°) for **4**[a,b]

Intramolecular distances			
Zr–Cl	2.4146(9)	C(1)–C(2)	1.419(4)
Zr–C(1)	2.465(3)	C(2)–C(3)	1.415(4)
Zr–C(2)	2.477(3)	C(3)–C(4)	1.406(4)
Zr–C(3)	2.633(3)	C(4)–C(9)	1.433(4)
Zr–C(4)	2.612(3)	C(9)–C(1)	1.413(4)
Zr–C(9)	2.519(3)	C(1)–C(10)	1.513(4)
Si–O	1.675(2)	Zr–Cen	2.2384(4)
C(3)–O	1.361(3)		
Intramolecular angles			
Cl–Zr–Cl*	98.73(6)	C(3)–O–Si	126.5(2)
Cen–Zr–Cen*	126.43(2)	O–Si–C(13)	104.0(1)
Cp–Cp*[c]	63.59		

[a] Symmetry transformations used to generate equivalent atoms: *, $-x$, y, $1/2-z$.
[b] Cen refers to the centroids of the C_5 rings and * denotes an atom or centroid related by the crystallographic twofold axis.
[c] Angle between the cyclopentadienyl planes.

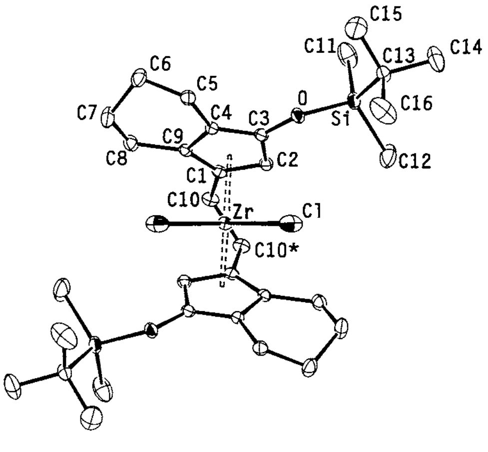

Fig. 2. Molecular structure of **4**. Thermal ellipsoids are drawn at 20% probability level.

Table 3
Selected bonding parameters for different siloxy-substituted bis(indenyl) and bis(tetrahydroindenyl) *ansa*-zirconocenes[a]

Zirconocene	Indenyl conformation	Zr–Cen (av) (Å)	Zr–Cl (av) (Å)	Cl–Zr–Cl (°)	Cen–Zr–Cen (°)	Cp–Cp (°)[b]	ηC–O (Å)	ref.
rac-Et(1-(*t*-BuMe$_2$SiO)IndH$_4$)$_2$ZrCl$_2$ (**4**)	Forward	2.238	2.415	98.7	126.40	63.60	1.361	This work
rac-Et(2-(*t*-BuMe$_2$SiO)IndH$_4$)$_2$ZrCl$_2$	Backward	2.231	2.439	98.20	125.20	58.60	1.376	[7]b
rac-Et(2-(iPr$_3$SiO)IndH$_4$)$_2$ZrCl$_2$	Backward	2.229	2.432	94.30	125.10	57.80	1.361	[7]d
rac-Et(2-(*t*-BuMe$_2$SiO)Ind)$_2$ZrCl$_2$	Backward	2.254	2.412	99.30	125.90	61.0	1.363	[7]a
rac-Et(2-(thexylMe$_2$SiO)Ind)$_2$ZrCl$_2$	Backward	2.243	2.433	97.90	120.30	58.6	1.356	[7]c
rac-Et(2-(iPr$_3$SiO)Ind)$_2$ZrCl$_2$	Forward	2.237	2.414	94.30	125.50	57.7	1.366	[7]d
meso-Et(1-(*t*-BuMe$_2$SiO)Ind)$_2$ZrCl$_2$ (**3b**)	Staggered	2.252	2.431	96.20	126.40	64.60	1.341	This work

[a] Cen refers to the centroids of the C_5 rings.

[b] Angle between the cyclopentadienyl planes.

observed for racemic silylene-bridged *ansa*-bis(indenyl)zirconium dichlorides (61.4–61.9°) [13]. This parameter is of particular importance in polymerization catalysis, as the corresponding increase in the coordination-gap aperture [14] generally improves the accessibility of the reaction center, and thus enhances the polymerization activity [13].

The oxygen-chlorine distance of **4** [3.161(4) Å] is shorter than the sum of their relevant van der Waals radii (3.20 Å). For **3b** the corresponding distances range from 3.15 to 3.30 Å with the former value affected by some conformational disorder. In both complexes the cyclopentadienyl-oxygen planes are, however, essentially planar. For **4**, distortion of the oxygen atom from the Cp-plane is approximately 0.018 Å. Intuitively, one could expect a stronger deviation caused by repulsion between the two electronegative atoms. Similar heteroatom-chlorine close contacts were observed for the unbridged dimethylamino-functionalized bis(cyclopentadienyl) [2] and bis(indenyl) [3]a metallocene dichlorides. The 2-siloxy-substituted complexes (see Table 3) appear to favor the indenyl-backward conformation in their solid state structures [7], which places the oxygen-chlorine atoms in a closer contact than in the corresponding indenyl-forward conformations. Electron overlap from the oxygen atom to the aromatic five-membered ring or the empty orbitals of the neighboring Si or Zr could result in a sufficient electron deficiency that allows or enhances these short intramolecular distances.

The detailed olefin homo- and copolymerization behavior of the new complexes is currently under investigation. Preliminary results show high ethylene polymerization activities at low [Al]:[Zr] ratios for both MAO-activated metallocenes **3a** and **4**. In polymerization of propylene, **3a**/MAO gives only atactic polypropylene with very low activity, whereas **4**/MAO appears to be practically inactive.

3. Experimental section

3.1. General comments

All operations with the organometallic reagents were carried out in an argon atmosphere using standard Schlenk techniques. Solvents were dried and distilled under argon prior to use. The ^{1}H and ^{13}C NMR spectra were recorded in $CDCl_3$ or CD_2Cl_2 solutions using a JEOL JNM-LA400 or JEOL JNM-A500 NMR spectrometer and referenced against tetramethylsilane or the residual protons of the deuterated solvents ($CHCl_3$ = 7.24 ppm, $CDHCl_2$ = 5.36 ppm). Direct inlet ionization mass spectra (EIMS) were obtained on a Varian-8000 mass spectrometer.

3.2. 3-(Tert-butyldimethylsiloxy)indene (**1**)

To a solution of *tert*-butyldimethylchlorosilane (125.7 g, 834 mmol) and 1-indanone (100.2 g, 758 mmol) in benzene (800 ml) at 0°C was added dropwise DBU (150.0 g, 985 mmol). The reaction mixture was stirred overnight at room temperature, diluted with Et_2O (400 ml), washed with water (2 × 500 ml) and dried over sodium sulfate. Evaporation of the solvents and distillation under reduced pressure gave 171.64 g (92%) of **1** as a yellow oil (b.p. 110–112°C/0.02 mbar).

^{1}H NMR ($CDCl_3$, δ): 7.40–7.35 (m, 2H); 7.30–7.26 (m, 1H); 7.21–7.17 (m, 1H); 5.39 (t, $^3J = 2.4$ Hz, 1H); 3.24 (d, $^3J = 2.4$ Hz, 2H); 1.02 (s, 9H); 0.24 (s, 6H). ^{13}C NMR ($CDCl_3$, δ): 153.72; 142.67; 141.90; 125.97; 125.06; 123.71; 118.12; 105.76; 33.88; 25.72; 18.21; −4.72.

3.3. Bis(3-(tert-butyldimethylsiloxy)-1-indenyl)ethane (**2**)

To a solution of **1** (49.28 g, 200.0 mmol) in THF (200 ml) at −30°C was added dropwise *n*-BuLi (80.8 ml of a 2.5 M solution in hexane, 202.0 mmol), and the reaction mixture was stirred overnight at room temperature. The resulting solution was cooled to −80°C and treated dropwise with a solution of dibromoethane (18.79 g, 100.0 mmol) in THF (100 ml). The reaction mixture was gradually warmed to room temperature, stirred overnight and washed with saturated ammonium chloride solution (300 ml). The organic phase was dried over sodium sulfate. Solvents were evaporated and the remaining oil was dissolved in pentane (200 ml). Concentration and cooling to −30°C gave 27.12 g (52%) of **2** as an-off white powder and 3:2 mixture of two diastereomers. Further concentration and cooling gave the second crop 5.43 g (11%) as an off-yellow powder enriched in the minor diastereomer. Total yield: 63%. EIMS (calcd/found): *m/e* 518.3036/518.3044.

^{1}H NMR ($CDCl_3$, δ): 7.34–7.18 (m, 8 + 8H, maj. + min. diast.); 5.38 (d, $^3J = 2.2$ Hz, 2H, maj. diast.); 5.37 (d, $^3J = 2.3$ Hz, 2H, min. diast.); 3.40–3.35 (m, 2 + 2H, maj. + min. diast.); 2.07–1.98 (m, AA′, 2H, maj. diast.); 1.84–1.79 (m, AA′, 2H, min. diast.); 1.65–1.60 (m, BB′, 2H, min. diast.); 1.45–1.36 (m, BB′, 2H, maj. diast.); 1.02 (s, 18H, min. diast.); 1.01 (s, 18H, maj. diast.); 0.25 (s, 6H, min. diast.); 0.23 (s, 6H, maj. diast.); 0.23 (s, 6 + 6H, maj. + min. diast.). ^{13}C NMR ($CDCl_3$, δ, maj. diast.): 153.24; 146.61; 141.52; 126.27; 125.32; 122.61; 118.18; 110.79; 45.53; 29.84; 25.73; 18.25; −4.67; −4.74. ^{13}C NMR ($CDCl_3$, δ, min. diast.): 153.19; 146.64; 141.56; 126.27; 125.31; 122.66; 118.18; 110.91; 45.48; 29.44; 25.73; 18.25; −4.65; −4.72.

3.4. *Rac- and meso-[ethylenebis(1-(tert-butyldimethylsiloxy)-3-indenyl)]zirconium dichlorides (**3a**,**3b**)*

To a solution of **2** (12.8 g, 24.7 mmol) in THF (70 ml) at −40°C was added dropwise *n*-BuLi (19.9 ml of a 2.5 M solution in hexane, 49.7 mmol), and the reaction mixture was stirred for 4 h at room temperature. The resulting dark red solution was added dropwise to a suspension of $ZrCl_4$ (5.76 g, 24.7 mmol) in THF (80 ml) at −60°C. The reaction mixture was gradually warmed to room temperature and stirred overnight. Evaporation of the solvents left a bright orange solid that was extracted with CH_2Cl_2 (150 ml) and filtrated through Celite to remove lithium chloride. The solvent was evaporated and the crude product was extracted with Et_2O (250 ml) and filtrated through Celite. Concentration and cooling to −30°C gave 4.09 g (20.1%) of **3** · 2THF as a 5:1 mixture of the *rac*- (**3a**) and *meso*- (**3b**) diastereomers as a bright orange powder. Further concentration and cooling gave the second crop 0.56 g (1.7%) of pure **3a** · 2THF. Samples of the pure racemic diastereomer, free of THF, were obtained as bright orange microcrystalline solids by careful recrystallization of the **3a**/**3b** · 2THF mixture from toluene. The collected mother liquors from the crystallizations were evaporated to dryness. Extraction of the Et_2O insolubles and the evaporated mother liquors with CH_2Cl_2 (200 ml) and the subsequent filtration through celite, concentration and cooling to −30°C gave 0.70 g (3.7%) of **3b** · CH_2Cl_2. Recrystallization from toluene gave pure **3b** as a dark orange/red microcrystalline solid. The EIMS mass spectra of both diastereomers show parent ions of composition $C_{32}H_{44}Si_2O_2ZrCl_2^+$ at $m/e = 676–684$ in the appropriate isotope ratios.

3a: ^{1}H NMR (CD_2Cl_2, δ): 7.39–7.34 (m, 4H); 7.14–7.10 (m, 2H); 7.04–7.00 (m, 2H); 5.60 (s, 2H); 3.77–3.67 (m, AA′, 2H); 3.49–3.39 (m, BB′, 2H); 0.97 (s, 18H); 0.21 (s, 6H); 0.19 (s, 6H). ^{13}C NMR (CD_2Cl_2, δ): 145.88; 126.55; 124.88; 122.48; 122.02; 121.38; 117.48; 111.09; 99.50; 28.69; 25.79; 18.65; −3.51; −4.32.

3b: ^{1}H NMR (CD_2Cl_2, δ): 7.45–7.43 (m, 2H); 7.36–7.34 (m, 2H); 7.04–7.01 (m, 2H); 6.98–6.94 (m, 2H); 5.72 (s, 2H); 4.01–3.93 (m, AA′, 2H); 3.51–3.43 (m, BB′, 2H); 1.02 (s, 18H); 0.32 (s, 6H); 0.23 (s, 6H). ^{13}C NMR (CD_2Cl_2, δ): 144.36; 126.71; 124.72; 122.59; 122.31; 121.84; 118.65; 110.84; 102.47; 30.10; 25.83; 18.71; −3.56; −4.31.

3.5. *Rac-[ethylenebis(1-(tert-butyldimethylsiloxy)-4,5,6,7-tetrahydro-3-indenyl)]zirconium dichloride (**4**)*

A 9:1 mixture of **3a** and **3b** (1.52 g, 2.24 mmol) and PtO_2 (20 mg) in CH_2Cl_2 (150 ml) was hydrogenated at 70 bar in a stirred reactor for 16 h. The light green suspension was filtrated through celite. Evaporation of the solvent left a light green solid that was dried in vacuo and dissolved in hexane (80 ml). Concentration and cooling to −30°C gave 1.28 g (84%) of a 9:1 mixture of **4** and its *meso*-diastereomer as a light green microcrystalline solid. Samples of pure **4** were obtained by careful recrystallization from the same solvent. In the EIMS mass spectrum of **4**, parent ions of composition $C_{32}H_{52}Si_2O_2ZrCl_2^+$ were observed at $m/e = 684–692$ in the appropriate isotope ratios. The base peak at $m/e = 627–635$ corresponds to M^+-*t*-Bu.

Table 4
Crystal data and structure refinement for **3b** and **4**

Empirical formula	$C_{32}H_{44}Cl_2O_2Si_2Zr$	$C_{16}H_{26}ClOSiZr_{1/2}$
fw	679.00	687.06
Temp (K)	293	293
Cryst size (mm)	0.20 × 0.15 × 0.10	0.18 × 0.22 × 0.34
Cryst appearence	Orange, prism	Yellow, plate
Cryst system	Monoclinic	Monoclinic
Space group	*P*121/*c*1	*C*2/c
Unit cell dimens (Å)	$a = 13.231(4)$ $b = 19.898(10)$ $c = 14.370(5)$ $\beta = 115.08(2)°$	$a = 27.810(2)$ $b = 12.219(3)$ $c = 11.348(2)$ $\beta = 113.74(1)°$
V(Å^3)	3426(2)	3530(1)
Z	4.00	8.00
d(calc) (g/cm^3)	1.316	1.293
μ(MoKα) (cm^{-1})	5.73	5.50
F(000)	1416.00	1448.00
R(int)	0.0875	0.013
Measured reflcns	4701.00	3346.00
Unique reflcns	4476.00	3273.00
Observed reflcns [$I > 3.00\sigma(I)$]		2514.00
Max and min transm coefficients	1.00 and 0.93	1.00 and 0.94
Goodness-of-fit indicator	0.989	2.11
Final R indices	$R = 0.069$, w$R = 0.144$	$R = 0.033$, w$R = 0.033$
Max and min $\Delta\rho$(e Å^{-3})	0.560 and −0.521	0.73 and −0.40

^{1}H NMR ($CDCl_3$, δ): 4.96 (s, 2H); 3.09–2.99 (m, AA′, 2H); 2.89–2.79 (m, BB′, 2H); 2.71–2.64 (m, 2H); 2.47–2.29 (m, 6H); 1.99–1.84 (m, 4H); 1.56–1.35 (m, 4H); 0.94 (s, 18H); 0.22 (s, 6H); 0.15 (s, 6H). ^{13}C NMR ($CDCl_3$, δ): 151.00; 121.61; 121.18; 116.04; 94.68; 27.66; 25.74; 23.47; 22.05; 21.89; 20.52; 18.33; −3.33; −4.20.

3.6. *X-ray structure determination*

Crystallographic data and parameters for **3b** and **4** are presented in Table 4. The data sets were collected on a Rigaku AFC5S diffractometer using Mo K$_\alpha$ radiation at 293 K. The intensities were corrected for Lorentz and polarization effects. The experimental absorption correction was carried out (ψ-scan). The structure of **3b** was solved by direct methods and refined by least squares techniques to the R value of 0.069 ($wR = 0.144$). One siloxy group of **3b** is disordered having two different orientations. Heavy atoms were refined with anisotropic displacement parameters. Hydrogen atoms were included in calculated positions with fixed displacement parameters (1.2 × that of the host atom). Hydrogen atoms of the disordered siloxy group were not included. The structure of **4** was solved by direct methods and refined by least squares techniques to the R value of 0.033 ($wR = 0.033$). Heavy atoms were refined with anisotropic displacement parameters. Hydrogen atoms were included in calculated positions with fixed displacement parameters (1.2 × that of the host atom) except those of the cyclopentadienyl ring and ethylene bridge, which were found from the Fourier map and were refined isotropically. Refinements were performed using SHELXS93 [15] (**3b**) and TEXSAN [16] (**4**) software. Figures were plotted on ORTEPII [17]. The atomic coordinates of **3b** and **4** are collected in Tables 5 and 6. Additional data including complete listings of crystal data and structure refinement, positional and thermal parameters and intramolecular distances and angles, and ORTEP views of **3b** and **4** are recorded as supplementary material and can be obtained from the authors upon request.

Table 5
Atomic coordinates ($\times 10^4$) and equivalent isotropic displacement parameters ($Å^2 \times 10^3$) for **3b**

Atom	x	y	z	U(eq)
Zr	296(1)	2160(1)	1094(1)	33(1)
Cl(1)	−499(3)	3185(2)	154(2)	56(1)
Cl(2)	449(3)	1572(2)	−327(2)	49(1)
Si(1A)	−3122(5)	3127(3)	1100(5)	50(2)
Si(1B)	−3691(11)	2814(8)	641(8)	59(6)
Si(2)	2014(3)	4374(2)	1804(2)	43(1)
O(1)	−2479(6)	2641(4)	589(5)	52(2)
O(2)	2123(6)	3573(3)	1532(6)	42(2)
C(1)	−319(9)	1481(6)	2175(8)	39(3)
C(2)	−900(8)	2110(6)	2051(7)	36(3)
C(3)	−1719(9)	2156(6)	1020(8)	42(3)
C(4)	−1669(9)	1550(6)	502(8)	36(3)
C(5)	−2351(9)	1311(7)	−521(8)	47(3)
C(6)	−2181(12)	684(7)	−770(10)	60(4)
C(7)	−1326(11)	273(6)	−59(10)	56(4)
C(8)	−644(10)	478(5)	886(8)	40(3)
C(9)	−817(9)	1125(6)	1223(9)	40(3)
C(10)	582(9)	1220(6)	3183(7)	45(3)
C(11)	1462(10)	1778(5)	3679(8)	44(3)
C(12)	1737(8)	2123(6)	2880(7)	33(3)
C(13)	1587(8)	2830(6)	2637(7)	35(3)
C(14)	2017(9)	2972(5)	1903(8)	35(3)
C(15)	2446(9)	2366(5)	1693(8)	39(3)
C(16)	3054(9)	2239(6)	1094(8)	48(3)
C(17)	3423(10)	1617(6)	1086(8)	51(3)
C(18)	3228(10)	1080(6)	1643(10)	61(4)
C(19)	2652(10)	1187(6)	2228(8)	45(3)
C(20)	2271(9)	1839(5)	2285(9)	39(3)
C(21)	−3487(13)	2593(7)	1995(8)	87(5)
C(22A)	−2187(16)	3857(8)	1729(16)	76(7)
C(22B)	−3000(4)	4070(3)	1210(3)	110(2)
C(23A)	−4435(9)	3353(7)	−80(8)	58(6)
C(23B)	−3970(16)	3731(9)	303(14)	64(15)
C(24)	−4065(12)	3765(9)	−808(11)	104(6)
C(25)	−5143(13)	3836(8)	262(13)	113(6)
C(26)	−5037(12)	2670(9)	−527(11)	140(8)
C(27)	790(10)	4506(6)	2109(10)	65(4)
C(28)	1784(11)	4819(6)	612(8)	68(4)
C(29)	3326(10)	4631(6)	2924(9)	54(3)
C(30)	3453(13)	4260(8)	3917(9)	102(6)
C(31)	4335(12)	4473(7)	2703(11)	96(5)
C(32)	3338(14)	5378(7)	3116(10)	106(6)

U(eq) is defined as one third of the trace of the orthogonalized U_{ij} tensor.

Table 6
Atomic coordinates and B(eq) for **4**

Atom	x	y	z	B(eq)
Zr	0.00	0.26172(3)	1/4	2.49(2)
Cl	0.07087(4)	0.39040(8)	0.3481(1)	5.84(5)
Si	0.16078(3)	0.24989(8)	0.17469(9)	3.72(4)
O	0.09881(7)	0.2947(2)	0.1247(2)	3.25(8)
C(1)	0.0032(1)	0.0959(2)	0.1297(3)	2.6(1)
C(2)	0.0550(1)	0.1387(2)	0.1821(3)	2.8(1)
C(3)	0.0560(1)	0.2341(2)	0.1125(3)	2.7(1)
C(4)	0.0046(1)	0.2573(2)	0.0246(2)	2.5(1)
C(5)	−0.0143(1)	0.3450(3)	−0.0760(3)	3.2(1)
C(6)	−0.0627(1)	0.3050(3)	−0.1907(3)	4.5(2)
C(7)	−0.1034(1)	0.2561(3)	−0.1511(4)	4.8(2)
C(8)	−0.0845(1)	0.1578(3)	−0.0616(3)	3.4(1)
C(9)	−0.0281(1)	0.1699(2)	0.0338(3)	2.4(1)
C(10)	−0.0121(1)	−0.0092(2)	0.1763(3)	3.1(1)
C(11)	0.1622(1)	0.1368(3)	0.0667(4)	6.7(2)
C(12)	0.1861(2)	0.2015(4)	0.3446(4)	8.3(2)
C(13)	0.1981(1)	0.3721(3)	0.1603(3)	3.9(1)
C(14)	0.2565(1)	0.3440(4)	0.2062(5)	7.4(2)
C(15)	0.1781(2)	0.4082(4)	0.0208(4)	8.4(3)
C(16)	0.1910(2)	0.4663(4)	0.2396(5)	9.1(3)

B(eq) is defined as $(8\pi^2/3)\Sigma_i\Sigma_j U_{ij}a_i^* a_j^* a_i a_j$.

Acknowledgements

Financial support from the Academy of Finland (RL) and the Finnish Technology Development Center (TEKES) (HL, PE, JN) is gratefully acknowledged. The authors wish to thank Mr. Markku Reunanen (EIMS), Mrs. Päivi Pennanen (NMR) and Dr. Reijo Sillanpää (X-ray) for their assistance in characterizing the products.

References

[1] For reviews, see: (a) P.C. Möhring, N.J. Coville, J. Organomet. Chem. 479 (1994) 1. (b) H.H. Brintzinger, D. Fischer, R. Mülhaupt, B. Rieger, R.M. Waymouth, Angew. Chem. Int. Ed. Engl. 34 (1995) 114. (c) M. Bochmann, J. Chem. Soc., Dalton Trans. (1996) 255. (d) W. Kaminsky, M. Arndt, Adv. Polym. Sci. 127 (1997) 143.

[2] K.-P. Stahl, G. Boche, W. Massa, J. Organomet. Chem. 277 (1984) 113.

[3] (a) H.J.G. Luttikhedde, R.P. Leino, C.-E. Wilén, J.H. Näsman, M.J. Ahlgrén, T.A. Pakkanen, Organometallics 15 (1996) 3092. (b) H. Plenio, D. Burth, J. Organomet. Chem. 519 (1996) 269. (c) E. Barsties, S. Schaible, M.-H. Prosenc, U. Rief, W. Röll, O. Weyand, B. Dorer, H.-H. Brintzinger, J. Organomet. Chem. 520 (1996) 63. (d) H.J.G. Luttikhedde, R. Leino, M.J. Ahlgrén, T.A. Pakkanen, J.H. Näsman, J. Organomet. Chem. 557 (1998) 225.

[4] J. Gräper, G. Paolucci, R.D. Fischer, J. Organomet. Chem. 501 (1995) 211.

[5] H. Naderer, E. Siebel, R.D. Fischer, J. Organomet. Chem. 518 (1996) 181.

[6] K.-H. Thiele, C. Schließburg, B. Neumüller, Z. Anorg. Allg. Chem. 621 (1995) 1106.

[7] (a) R. Leino, H. Luttikhedde, C.-E. Wilén, R. Sillanpää, J.H. Näsman, Organometallics 15 (1996) 2450. (b) R. Leino, H.J.G. Luttikhedde, P. Lehmus, C.-E. Wilén, R. Sjöholm, A. Lehtonen, J.V. Seppälä, J.H. Näsman, Macromolecules 30 (1997) 3477. (c) R. Leino, H.J.G. Luttikhedde, P. Lehmus, C.-E. Wilén, R. Sjöholm, A. Lehtonen, J.V. Seppälä, J.H. Näsman, J. Organomet. Chem., submitted (d) H.J.G. Luttikhedde, R. Leino, A. Lehtonen, J.H. Näsman, J. Organomet. Chem. 555 (1998) 127.

[8] F. Piemontesi, I. Camurati, L. Resconi, D. Balboni, A. Sironi, M. Moret, R. Zeigler, N. Piccolrovazzi, Organometallics 14 (1995) 1256.

[9] S. Collins, B.A. Kuntz, N.J. Taylor, D.G. Ward, J. Organomet. Chem. 342 (1988) 21.

[10] S. Collins, W.J. Gauthier, D.A. Holden, B.A. Kuntz, N.J. Taylor, D.G. Ward, Organometallics 10 (1991) 2061.

[11] L. Resconi, F. Piemontesi, I. Camurati, D. Balboni, A. Sironi, M. Moret, H. Rychlicki, R. Zeigler, Organometallics 15 (1996) 5046.

[12] J.A. Ewen, M.J. Elder, R.L. Jones, L. Haspeslagh, J.L. Atwood, S.G. Bott, K. Robinson, Makromol. Chem. Macromol. Symp. 48/49 (1991) 253.

[13] (a) W.A. Herrmann, J. Rohrmann, E. Herdtweck, W. Spaleck, A. Winter, Angew. Chem. Int. Ed. Engl. 28 (1989) 1511. (b) W. Spaleck, M. Antberg, J. Rohrmann, A. Winter, B. Bachmann, P. Kiprof, J. Behm, W.A. Herrmann, Angew. Chem. Int. Ed. Engl. 31 (1992) 1347.

[14] K. Hortmann, H.-H. Brintzinger, New J. Chem. 16 (1992) 51.

[15] G.M. Sheldrick, SHELXL93, Program for the Refinement of Crystal Structures, University of Göttingen, Germany, 1993.

[16] TEXSAN-TEXRAY, Structure Analysis Package, Molecular Structure Corporation, Houston, TX, 1989.

[17] C.K. Johnson, ORTEPII, Report ORNL-5138, Oak Ridge National Laboratory, Oak Ridge, TN, 1976.